Hydrogen-Evolution Catalysts

DOI: 10.1002/ange.201404161

Carbon Nanotubes Decorated with CoP Nanocrystals: A Highly Active Non-Noble-Metal Nanohybrid Electrocatalyst for Hydrogen Evolution**

*Qian Liu, Jingqi Tian, Wei Cui, Ping Jiang, Ningyan Cheng, Abdullah M. Asiri, and Xuping Sun**

Abstract: *The development of effective and inexpensive hydrogen evolution reaction (HER) electrocatalysts for future renewable energy systems is highly desired. The strongly acidic conditions in proton exchange membranes create a need for acid-stable HER catalysts. A nanohybrid that consists of carbon nanotubes decorated with CoP nanocrystals (CoP/CNT) was prepared by the low-temperature phosphidation of a Co_3O_4/CNT precursor. As a novel non-noble-metal HER catalyst operating in acidic electrolytes, the nanohybrid exhibits an onset overpotential of as low as 40 mV, a Tafel slope of 54 mV dec^{-1}, an exchange current density of 0.13 mA cm^{-2}, and a Faradaic efficiency of nearly 100 %. This catalyst maintains its catalytic activity for at least 18 hours and only requires overpotentials of 70 and 122 mV to attain current densities of 2 and 10 mA cm^{-2}, respectively.*

Hydrogen has been proposed as the principal energy carrier in the hydrogen-economy paradigm.[1] Electrolysis of water is the simplest way to produce hydrogen. To increase the reaction rate and lower the overpotential, it is necessary to use an efficient hydrogen evolution reaction (HER) electrocatalyst. Platinum group metals are the best HER catalysts, but they suffer from high cost.[2] Although abundant nickel-based alloys are often used as commercial HER catalysts,[3] they are not stable in acidic media and thus lack compatibility with electrolysis units that are based on proton exchange membranes.[4] These limitations have motivated significant efforts towards the design and development of acid-stable non-noble-metal HER catalysts, and huge progress has been made in this direction in the past few years. Molybdenum-based compounds are an exciting family of such catalysts that have been intensively studied, including MoS_2,[5] amorphous MoS_x,[6] $MoSe_2$,[7] MoB,[8] Mo_2C,[8,9] $NiMoN_x$,[10] and $Co_{0.6}Mo_{1.4}N_2$.[11]

Transition-metal phosphides (TMPs) are an important class of compounds that are formed by the alloying of metals and phosphorus.[12] They have been used as anode materials for Li-ion batteries (LIBs)[13] and even more intensively as efficient catalysts for the hydrodesulfurization (HDS) reaction.[12–14] As both HDS and HER rely on the reversible binding of hydrogen to the catalyst (with hydrogen dissociation to yield H_2S in HDS and with protons bound to the catalyst to promote hydrogen formation in HER),[15] it is expected that TMPs may function as HER catalysts. Indeed, Ni_2P nanoparticles and FeP nanosheets have recently been shown to be active catalysts for the electrochemical hydrogen evolution from water.[16]

On the other hand, the electrocatalytic efficiency is also affected by the morphology and electrical conductivity of the catalyst.[17] The use of conductive carbon as the support material cannot only improve the conductivity of the hybrid catalyst, but also increases the dispersion of the active phases, so that the catalyst offers more active sites.[18] Herein, we present our recent efforts in developing a nanohybrid that consists of carbon nanotubes decorated with CoP nanocrystals (CoP/CNT) by the low-temperature phosphidation of its Co_3O_4/CNT precursor. Remarkably, when used as a non-noble-metal HER catalyst, this nanohybrid maintained its activity for at least 18 hours under acidic conditions with a Faradaic efficiency (FE) of nearly 100 % and exhibited an onset overpotential of 40 mV, a Tafel slope of 54 mV/dec, and an exchange current density of 0.13 mA cm^{-2}. Overpotentials of 70 and 122 mV were needed to drive current densities of 2 and 10 mA cm^{-2}, respectively.

Figure 1 shows the X-ray diffraction (XRD) patterns of CNT, Co_3O_4/CNT, and CoP/CNT. The CNT (curve a) shows two peaks at 26° and 43°, which were indexed to the (002) and (101) reflections of hexagonal graphite, respectively.[19] In contrast, the Co_3O_4/CNT material (curve b) shows six additional peaks at 31°, 37°, 45°, 56°, 59°, and 65°, which were indexed to the (220), (311), (400), (422), (511), and (440) planes of Co_3O_4, respectively (JCPDS 42-1467).[20] The great suppression of the strong (002) peak of CNT can be attributed to the loading of Co_3O_4 with high density. After phosphidation, only the diffraction peaks of the CoP phase are observed at 32°, 36°, 46°, 48°, 52°, and 57°, which were indexed to the (011), (111), (112), (211), (103), and (301) planes of CoP

[*] Q. Liu, Dr. J. Tian, W. Cui, Dr. P. Jiang, N. Cheng, Prof. X. Sun
State Key Laboratory of Electroanalytical Chemistry
Changchun Institute of Applied Chemistry
Changchun 130022, Jilin (China)
E-mail: sunxp@ciac.ac.cn
Dr. J. Tian, W. Cui, N. Cheng
Graduate School of the Chinese Academy of Sciences
Beijing 100039 (China)
Prof. A. M. Asiri, Prof. X. Sun
Chemistry Department & Center of Excellence for Advanced Materials Research, King Abdulaziz University
Jeddah 21589 (Saudi Arabia)

[**] This work was supported by the National Natural Science Foundation of China (21175129) and the National Basic Research Program of China (2011CB935800).

Supporting information for this article is available on the WWW under http://dx.doi.org/10.1002/anie.201404161.

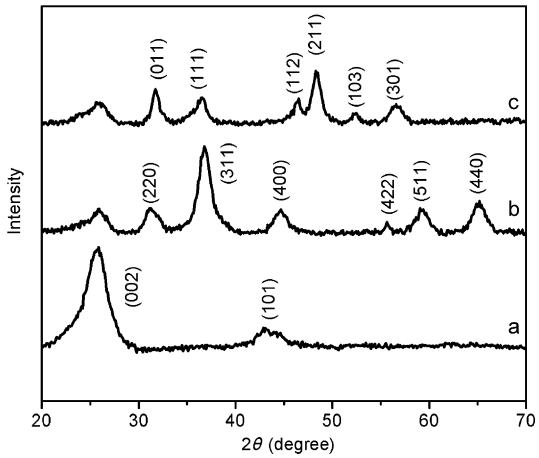

Figure 1. a–c) XRD patterns for CNT (a), Co_3O_4/CNT (b), and CoP/CNT (c).

(JCPDS-29-0497), respectively.[21] These observations suggest the successful chemical conversion of Co_3O_4 into CoP.

A transmission electron microscopy (TEM) image of the Co_3O_4/CNT hybrid reveals that the Co_3O_4 nanocrystals with a diameter of about 2–3 nm are distributed well on the CNT with high density (Figure 2a). A high-resolution TEM (HRTEM) image that was taken of one single nanocrystal shows the lattice fringes with d spacings of 0.46 and 0.24 nm, which correspond to the (111) and (311) plane of the Co_3O_4

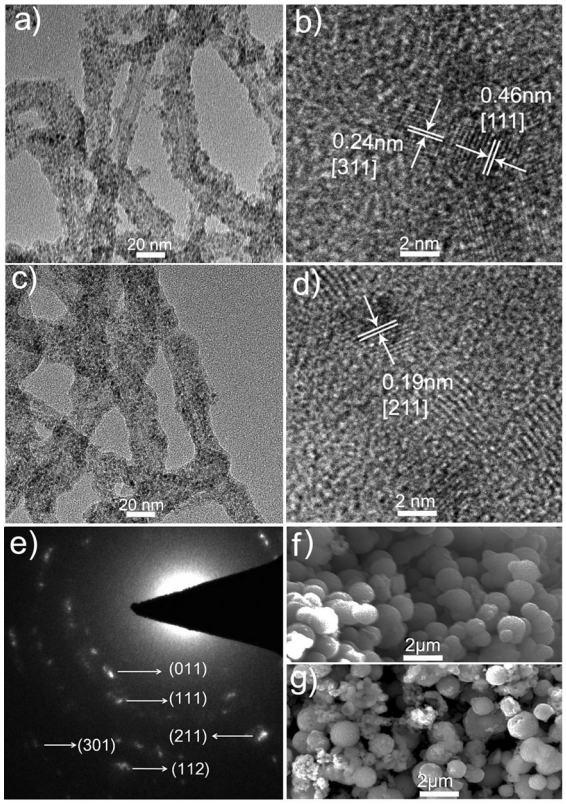

Figure 2. a) TEM and b) HRTEM images of Co_3O_4/CNT. c) TEM and d) HRTEM images of CoP/CNT. e) SAED pattern for CoP nanocrystals. SEM images of f) Co_3O_4 and g) CoP microspheres.

nanocrystals, respectively (Figure 2b).[20] After phosphidation, the size of these nanocrystals and the integration of the nanohybrid are well preserved (Figure 2c). The HRTEM image taken for one such nanocrystal reveals lattice fringes with a d spacing of 0.19 nm, which corresponds to the (211) plane of CoP (Figure 2d).[22] The corresponding selective area electron diffraction (SAED) pattern shows several bright rings that are made up of discrete spots, which can be indexed to the (011), (111), (112), (211), and (301) planes of orthorhombic CoP[23] (Figure 2e; see also the Supporting Information, Figure S1). The energy-dispersive X-ray (EDX) spectrum of these nanocrystals suggests that the cobalt/phosphorus atomic ratio is close to 1:1 (Figure S2). All of these results strongly support the formation of CoP/CNT nanocrystals from Co_3O_4/CNT by the low-temperature phosphidation reaction. When the same preparation procedure was repeated without CNTs, only Co_3O_4 microspheres were obtained (Figure 2f; see also Figure S3a), indicating that the CNTs are key to the generation of small Co_3O_4 nanocrystals. The following phosphidation yielded CoP microspheres (Figure 2g; see also Figure S3b).

To examine their electrocatalytic HER activities, CoP/CNT and CoP microspheres were deposited with the same loading of approximately 0.285 mg cm^{-2} on glassy carbon electrodes (GCEs), and the HER activities were measured in H_2SO_4 solution (0.5 M) using a typical three-electrode setup. For comparison, bare GCE, CNT, and commercial Pt/C (20 wt%) were also examined. Figure 3a shows the polarization curves without IR compensation. As expected, the Pt/C catalyst exhibited excellent HER activity with an overpotential close to zero. We also prepared a Pt/CNT material as another reference catalyst and found that while it also exhibited an overpotential close to zero, it could approach higher current densities than Pt/C at the same overpotential (Figure S4). Both bare GCE and CNT show very poor HER performance. It is surprising that the CoP microspheres show a large cathodic current density with a small onset overpotential of 100 mV for the HER, suggesting that the CoP particles are a very active HER catalyst. CoP/CNT exhibited a much smaller onset overpotential of 40 mV and achieved current densities of 2 and 10 mA cm^{-2} at overpotentials of 70 and 122 mV, respectively, whereas CoP microspheres needed an overpotential of 226 mV to reach a current density of 10 mA cm^{-2}. These values for CoP/CNT compare favorably to the behavior of other non-noble-metal HER catalysts in acidic media, such as MoS_2/RGO,[5d] double-gyroid MoS_2,[5e] metallic MoS_2 nanosheets,[5h] defect-rich MoS_2,[5i] MoS_2/graphene/Ni foam,[5j] MoS_2/MoO_3,[5k] MoS_3 film,[6a] bulk Mo_2C and Mo_2B,[8] Mo_2C/CNT,[9a] Mo_2C/GCS,[9b] $NiMoN_x$/C,[10] $Co_{0.6}Mo_{1.4}N_2$,[11] FeP nanosheets,[16b] and Co-NRCNTs[24] (Table S1). In addition, CoP/CNT shows an exchange current density of 0.13 mA cm^{-2} (Figure S5). Although this value is lower than that of Pt/C (0.76 mA cm^{-2}), it is higher than that of CoP microspheres (0.019 mA cm^{-2}) and most reported values for non-noble-metal HER catalysts, which are listed in Table S1. Figure S6 shows an optical photograph of the CoP/CNT nanohybrid on the GCE during a linear sweep voltammetry (LSV) scan, indicating the production of many hydrogen bubbles on the

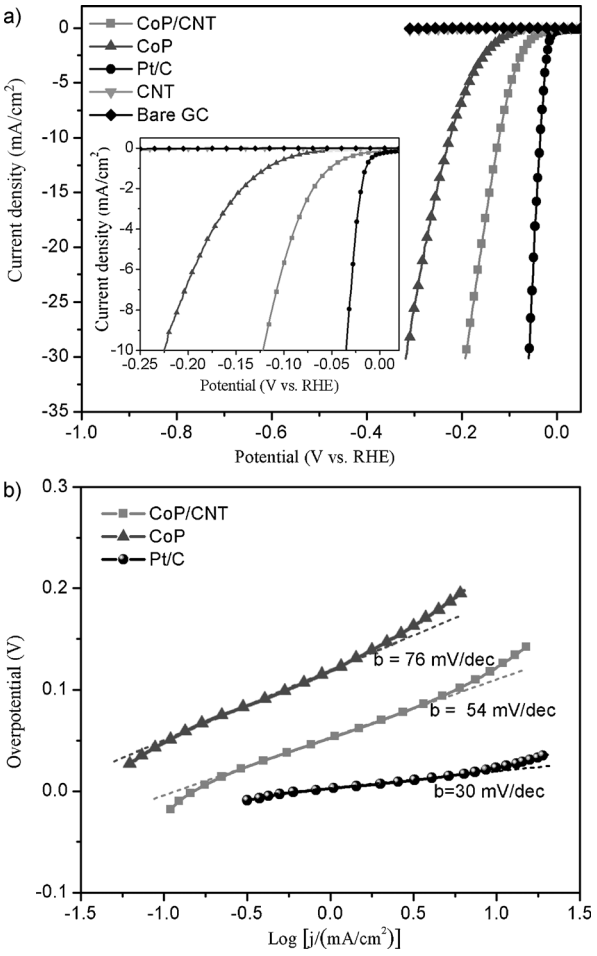

Figure 3. a) Polarization curves for CoP/CNT, CoP, CNT, Pt/C, and bare GCE in H_2SO_4 solution (0.5 M) at a scan rate of 2 $mV s^{-1}$. b) Tafel plots of CoP/CNT, CoP, and Pt/C.

electrode surface. Note that nanoporous CoP nanowire arrays supported on carbon cloth as an integrated 3D hydrogen evolution cathode only need 67 mV to afford a current density of 10 $mA cm^{-2}$ but with a higher exchange current density of 0.288 $mA cm^{-2}$ as compared to CoP/CNT.[25]

Tafel plots are shown in Figure 2b. These Tafel plots were fit to the Tafel equation ($\eta = b \log j + a$, where j is the current density and b is the Tafel slope), yielding Tafel slopes of approximately 30, 76, and 54 $mV dec^{-1}$ for Pt/C, CoP, and CoP/CNT, respectively. The measured Tafel slope for the Pt/C catalyst is close to the reported value for a commercial Pt catalyst.[16a] These Tafel slopes for both CoP catalysts do not match the expected Tafel slopes of 29, 38, and 116 $mV dec^{-1}$ correlating with a different rate-determining step of the HER,[16a] revealing that the HER proceeds through a Volmer–Heyrovsky mechanism.[26]

The observation of the superior HER activity of the CoP/CNT nanohybrid over the CoP microspheres can be attributed to the following two reasons. First, the small size of the CoP nanocrystals in the hybrid favors the exposure of more active sites for the HER. Second, the excellent electrical conductivity of the CNT support facilitates charge transfer in the hybrid. Indeed, electrochemical impedance spectroscopy measurements indicate that CoP/CNT has a much lower impedance and thus markedly faster HER kinetics than CoP (Figure S7).[27] To further verify this hypothesis, we prepared another control sample using polydopamine (PDA) spheres as a non-conductive support[28] (Figure S8). As expected, the PDA material that had been decorated with small CoP nanocrystals (CoP/PDA) exhibited a much lower HER activity (Figure S9) and a much larger impedance than CoP/CNT (Figure S7).

For practical applications, electrocatalysts are require to have high durability. For this reason, we further probed the durability of the CoP/CNT and CoP catalysts in acidic media by long-term cycling tests. The LSV curves that were measured for CoP/CNT before and after 2000 cyclic voltammetry (CV) cycles ranging from +0.081 to −0.32 V vs. RHE at a scan rate of 100 $mV s^{-1}$ are shown in Figure 4. At the end

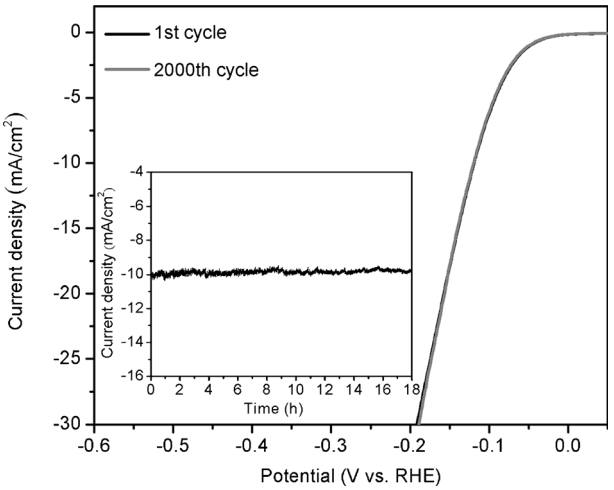

Figure 4. Polarization curves for CoP/CNT in H_2SO_4 solution (0.5 M) with a scan rate of 2 $mV s^{-1}$ before and after 2000 cycles at a scan rate of 100 $mV s^{-1}$ between +0.081 and −0.32 V. Inset: time dependence of the current density for CoP/CNT at a static overpotential of 122 mV for 18 hours.

of the cycling experiment, the LSV curve exhibits negligible loss in current density compared to the initial curve. In contrast, for CoP, a significant loss of current density had occurred after the 2000 cycles (Figure S10). The inset in Figure 4 shows the time dependence of the current density for CoP/CNT at an overpotential of 122 mV, suggesting that the nanohybrid maintained its catalytic activity for at least 18 hours. For CoP, however, only approximately 81% of the current density were maintained in the same period of time (Figure S10, inset). These results suggest that CoP/CNT is of superior stability in a long-term electrochemical process compared to CoP, amorphous MoS_2,[5f,g] defect-rich ultrathin MoS_2 nanosheets,[5i] and Ni_2P nanoparticles.[16a]

Gas generation was confirmed by gas chromatography (GC) analysis. The generated hydrogen was further measured quantitatively using a calibrated pressure sensor to monitor the pressure change in the cathode compartment of the H-type electrolytic cell. Potentiostatic cathodic electrolysis was performed by maintaining the glassy carbon plate loaded

with CoP/CNT at −0.25 V for 120 minutes. The FE of the electrocatalytic hydrogen evolution process was calculated by comparing the experimentally determined and theoretically calculated amounts of hydrogen (assuming 100% FE). The agreement of both values suggests that the FE is close to 100%, as shown in Figure 5.

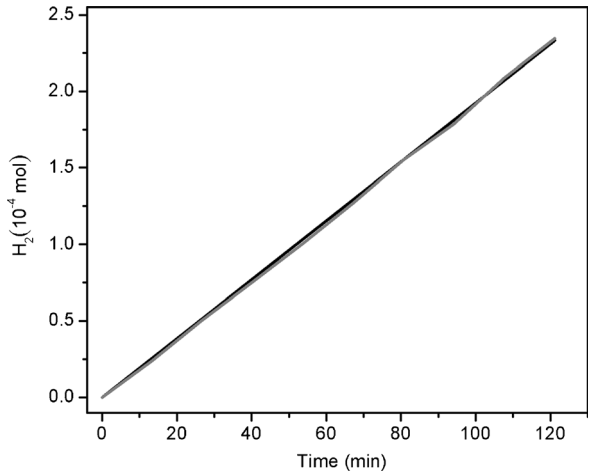

Figure 5. The theoretically calculated (black line) and experimentally measured (gray line) amount of evolved hydrogen versus time for the CoP/CNT hybrid at −0.25 V.

The Co($2p_{3/2}$) and P(2p) regions of the X-ray photoelectron spectroscopy (XPS) 2p spectrum of the CoP sample are shown in Figure S11a and S11b, respectively. Two peaks are apparent in the Co($2p_{3/2}$) region at 779.1 and 782.1 eV. A high-resolution image of the P(2p) region shows two peaks at 130.6 and 129.8 eV, reflecting the binding energy (BE) of P$2p_{1/2}$ and P$2p_{3/2}$, respectively, along with one peak at 134.6 eV, and the peaks at 779.1 and 129.8 eV are close to the BEs for Co and P in CoP.[29] The peaks at 782.1 and 134.6 eV are assigned to oxidized cobalt and phosphorus species, which arise from superficial oxidation of CoP because of air contact.[30] An XPS survey spectrum (Figure S11c) confirmed the presence of oxygen in the sample. The Co$2p_{3/2}$ BE of 779.1 eV is positively shifted from that of Co metal (778.1–778.2 eV), but the P$2p_{3/2}$ BE of 129.8 eV is negatively shifted from that of elemental P (130.2 eV).[31] This suggests that the cobalt in CoP has a partial positive charge (δ^+), while the phosphorus has a partial negative charge (δ^-), implying a transfer of electron density from Co to P.[29,32] Previous calculations and electron-density maps have also suggested that the Co–P bonds have a covalent character with charge separation that is due to charge transfer from Co to P.[29,33] For metal complex HER catalysts, they incorporate proton relays from pendant acidic or basic groups that are positioned close to the metal center where H_2 production occurs.[34] Hydrogenases also use pendant bases that are proximate to the metal centers as active sites.[35] Like metal complex catalysts and hydrogenases, the surface of the CoP nanocrystal also features pendant basic phosphorus centers (δ^-) in close proximity to the cobalt metal centers (δ^+). Therefore, the mechanism of the HER in the presence of a CoP catalyst is in principle similar to that with the metal complex catalysts and hydrogenases. Specifically, cobalt serves as the active center.[34–36] The cobalt centers and the basic phosphorus act as the hydride-acceptor and proton-acceptor centers, respectively, which facilitates the HER.[15c,16a] Such phosphorus centers could also facilitate the formation of cobalt hydride species for subsequent hydrogen evolution by electrochemical desorption.[37]

In summary, low-temperature phosphidation of Co_3O_4/CNT has been shown to be an effective preparative method for a CoP/CNT nanohybrid. This hybrid exhibits a superior HER catalytic activity, with a small onset overpotential of 40 mV, a Tafel slope of 54 mV dec^{-1}, and an exchange current density of 0.13 mA cm^{-2}. Furthermore, it requires overpotentials of 70 and 122 mV to attain current densities of 2 and 10 mA cm^{-2}, respectively, and its catalytic activity can be maintained for at least 18 hours. Our present study is important for three reasons: 1) An inexpensive acid-stable HER catalyst with high activity has been developed; 2) such hybrids hold great promise as catalysts for hydrodesulfurization and as anode materials for LIBs;[12–14] and 3) a general method for the mild preparation of nanohybrids that are based on transition-metal phosphides and carbon is provided.

Received: April 10, 2014
Published online: May 20, 2014

Keywords: carbon nanotubes · cobalt nanocrystals · electrolysis · heterogeneous catalysis · hydrogen evolution reaction

[1] D. A. J. Rand, R. M. Dell, *Hydrogen Energy: Challenges and Prospects*, RSC Publishing, Cambridge, **2007**.
[2] M. G. Walter, E. L. Warren, J. R. McKone, S. W. Boettcher, Q. Mi, E. A. Santori, N. S. Lewis, *Chem. Rev.* **2010**, *110*, 6446.
[3] a) D. E. Brown, M. N. Mahmood, M. C. M. Man, A. K. Turner, *Electrochim. Acta* **1984**, *29*, 1551; b) I. A. Raj, K. I. Vasu, *J. Appl. Electrochem.* **1990**, *20*, 32.
[4] a) G. A. Le, V. Artero, B. Jousselme, P. D. Tran, N. Guillet, R. Métayé, A. Fihri, S. Palacin, M. Fontecave, *Science* **2009**, *326*, 1384; b) M. Hambourger, M. Gervaldo, D. Svedruzic, P. W. King, D. Gust, M. Ghirardi, A. L. Moore, T. A. Moore, *J. Am. Chem. Soc.* **2008**, *130*, 2015.
[5] For examples, see : a) B. Hinnemann, P. G. Moses, J. Bonde, K. P. Jørgensen, J. H. Nielsen, S. Horch, I. Chorkendorff, J. K. Nørskov, *J. Am. Chem. Soc.* **2005**, *127*, 5308; b) T. F. Jaramillo, K. P. Jørgensen, J. Bonde, J. H. Nielsen, S. Horch, I. Chorkendorff, *Science* **2007**, *317*, 100; c) D. Merki, X. Hu, *Energy Environ. Sci.* **2011**, *4*, 3878; d) Y. Li, H. Wang, L. Xie, Y. Liang, G. Hong, H. Dai, *J. Am. Chem. Soc.* **2011**, *133*, 7296; e) J. Kibsgaard, Z. Chen, B. N. Reinecke, T. F. Jaramillo, *Nat. Mater.* **2012**, *11*, 963; f) J. D. Benck, Z. Chen, L. Y. Kuritzky, A. J. Forman, T. F. Jaramillo, *ACS Catal.* **2012**, *2*, 1916; g) A. B. Laursen, P. C. K. Vesborg, I. Chorkendorff, *Chem. Commun.* **2013**, *49*, 4965; h) M. A. Lukowski, A. S. Daniel, F. Meng, A. Forticaux, L. Li, S. Jin, *J. Am. Chem. Soc.* **2013**, *135*, 10274; i) J. Xie, H. Zhang, S. Li, R. Wang, X. Sun, M. Zhou, J. Zhou, X. Lou, Y. Xie, *Adv. Mater.* **2013**, *25*, 5807; j) Y. Chang, C. Lin, T. Chen, C. L. Hsu, Y. Lee, W. Zhang, K. Wei, L. Li, *Adv. Mater.* **2013**, *25*, 756; k) Z. Chen, D. Cummins, B. N. Reinecke, E. Clark, M. K. Sunkara, T. F. Jaramillo, *Nano Lett.* **2011**, *11*, 4168.

[6] a) D. Merki, S. Fierro, H. Vrubel, X. Hu, *Chem. Sci.* **2011**, *2*, 1262; b) H. Vrubel, D. Merki, X. Hu, *Energy Environ. Sci.* **2011**, *5*, 6136; c) D. Merki, H. Vrubel, L. Rovelli, S. Fierro, X. Hu, *Chem. Sci.* **2012**, *3*, 2515.
[7] a) D. Kong, H. Wang, J. J. Cha, M. Pasta, K. J. Koski, J. Yao, Y. Cui, *Nano Lett.* **2013**, *13*, 1341; b) H. Wang, D. Kong, P. Johanes, J. J. Cha, G. Zheng, K. Yan, N. Liu, Y. Cui, *Nano Lett.* **2013**, *13*, 3426.
[8] H. Vrubel, X. Hu, *Angew. Chem.* **2012**, *124*, 12875; *Angew. Chem. Int. Ed.* **2012**, *51*, 12703.
[9] a) W. Chen, C. Wang, K. Sasaki, N. Marinkovic, W. Xu, J. T. Muckerman, Y. Zhu, R. R. Adzic, *Energy Environ. Sci.* **2013**, *6*, 943; b) W. Cui, N. Cheng, Q. Liu, C. Ge, Z. Xing, A. M. Asiri, A. Y. Obaid, X. Sun, unpublished results.
[10] W. Chen, K. Sasaki, C. Ma, A. I. Frenkel, N. Marinkovic, J. T. Muckerman, Y. Zhu, R. R. Adzic, *Angew. Chem.* **2012**, *124*, 6235; *Angew. Chem. Int. Ed.* **2012**, *51*, 6131.
[11] B. Cao, G. M. Veith, J. C. Neuefeind, R. R. Adzic, P. G. Khalifah, *J. Am. Chem. Soc.* **2013**, *135*, 19186.
[12] S. T. Oyama, T. Gott, H. Zhao, Y.-K. Lee, *Catal. Today* **2009**, *143*, 94.
[13] S. Carenco, D. Portehault, C. Boissière, N. Mézailles, C. Sanchez, *Chem. Rev.* **2013**, *113*, 7981.
[14] R. Prins, M. E. Bussell, *Catal. Lett.* **2012**, *142*, 1413.
[15] a) J. O. M. Bockris, E. C. Potter, *J. Electrochem. Soc.* **1952**, *99*, 169; b) P. Liu, J. A. Rodriguez, T. Asakura, J. Gomes, K. Nakamura, *J. Phys. Chem. B* **2005**, *109*, 4575; c) P. Liu, J. A. Rodriguez, *J. Am. Chem. Soc.* **2005**, *127*, 14871.
[16] a) E. J. Popczun, J. R. McKone, C. G. Read, A. J. Biacchi, A. M. Wiltrout, N. S. Lewis, R. E. Schaak, *J. Am. Chem. Soc.* **2013**, *135*, 9267; b) Y. Xu, R. Wu, J. Zhang, Y. Shi, B. Zhang, *Chem. Commun.* **2013**, *49*, 6656.
[17] L. Liao, J. Zhu, X. Bian, L. Zhu, M. D. Scanlon, H. H. Girault, B. Liu, *Adv. Funct. Mater.* **2013**, *23*, 5326.
[18] a) K. P. de Jong, *Curr. Opin. Solid State Mater. Sci.* **1999**, *4*, 55; b) Y. Liang, Y. Li, H. Wang, H. Dai, *J. Am. Chem. Soc.* **2013**, *135*, 2013; c) H. Huang, X. Wang, *J. Mater. Chem. A* **2014**, *2*, 6266.
[19] a) Q. Zhu, A. N. A. Sujari, S. A. Ghani, *J. Electrochem. Soc.* **2013**, *160*, 23; b) Z. Lu, H. Wang, *CrystEngComm* **2014**, *16*, 550.
[20] a) C. Xu, J. Sun, L. Gao, *CrystEngComm* **2011**, *13*, 1586; b) S. Chen, Y. Wang, *J. Mater. Chem.* **2010**, *20*, 9735.
[21] A. Infantes-Molina, J. A. Cecilia, B. Pawelec, J. L. G. Fierro, E. Rodríguez-Castellón, A. Jiménez-López, *Appl. Catal. A* **2010**, *390*, 253.
[22] W. Maneeprakorn, M. A. Malik, P. O'Brien, *J. Mater. Chem.* **2010**, *20*, 2329.
[23] a) Y. Li, M. A. Malik, P. O'Brien, *J. Am. Chem. Soc.* **2005**, *127*, 16020; b) Y. Cui, M. Xue, Z. Fu, X. Wang, X. Liu, *J. Alloys Compd.* **2013**, *555*, 283.
[24] X. Zou, X. Huang, A. Goswami, R. Silva, B. R. Sathe, E. Mikmekova, T. Asefa, *Angew. Chem.* **2014**, *126*, 4461; *Angew. Chem. Int. Ed.* **2014**, *53*, 4372.
[25] J. Tian, Q. Liu, A. M. Asiri, X. Sun, *J. Am. Chem. Soc.* **2014**, DOI: 10.1021/ja503372r.
[26] a) N. Pentland, J. O. M. Bockris, E. Sheldon, *J. Electrochem. Soc.* **1957**, *104*, 182; b) B. E. Conway, B. V. Tilak, *Electrochim. Acta* **2002**, *47*, 3571.
[27] C. Guo, L. Zhang, J. Miao, J. Zhang, C. M. Li, *Adv. Energy Mater.* **2013**, *3*, 167.
[28] D. Del Frari, J. Bour, V. Ball, V. Toniazzo, D. Ruch, *Polym. Degrad. Stab.* **2012**, *97*, 1844.
[29] A. P. Grosvenor, S. D. Wik, R. G. Cavell, A. Mar, *Inorg. Chem.* **2005**, *44*, 8988.
[30] a) T. Korányi, *Appl. Catal. A* **2003**, *239*, 253; b) S. J. Sawhill, K. A. Layman, D. R. Van Wyk, M. H. Engelhard, C. Wang, M. E. Bussell, *J. Catal.* **2005**, *231*, 300; c) H. Li, P. Yang, D. Chu, H. Li, *Appl. Catal. A* **2007**, *325*, 34; d) J. Wang, Q. Yang, Z. Zhang, S. Sun, *Chem. Eur. J.* **2010**, *16*, 7916.
[31] *Practical Surface Analysis by Auger and X-ray Photoelectron Spectroscopy* (Eds.: D. Briggs, M. P. Seah), Wiley, New York, **1983**.
[32] A. W. Burns, K. A. Layman, D. H. Bale, M. E. Bussell, *Appl. Catal. A* **2008**, *343*, 68.
[33] a) Z. Yang, L. Liu, X. Wang, S. Yang, X. Su, *J. Alloys Compd.* **2011**, *509*, 165; b) S. Diplas, Ø. Prytz, O. B. Karlsen, J. F. Watts, J. Taftø, *J. Phys. Condens. Matter* **2007**, *19*, 246216.
[34] a) A. D. Wilson, R. H. Newell, M. J. McNevin, J. T. Muckerman, M. R. Dubois, D. L. Dubois, *J. Am. Chem. Soc.* **2006**, *128*, 358; b) A. D. Wilson, R. K. Shoemaker, A. Miedaner, J. T. Muckerman, D. L. Dubois, M. R. Dubois, *Proc. Natl. Acad. Sci. USA* **2007**, *104*, 6951; c) B. E. Barton, T. B. Rauchfuss, *J. Am. Chem. Soc.* **2010**, *132*, 14877.
[35] Y. Nicolet, A. L. de Lacey, X. Vérnede, V. M. Fernandez, E. C. Hatchikian, J. C. Fontecilla-Camps, *J. Am. Chem. Soc.* **2001**, *123*, 1596.
[36] a) J. L. Dempsey, B. S. Brunschwig, J. R. Winkler, H. B. Gray, *Acc. Chem. Res.* **2009**, *42*, 1995; b) V. Artero, M. Chavarot-Kerlidou, M. Fontecave, *Angew. Chem.* **2011**, *123*, 7376; *Angew. Chem. Int. Ed.* **2011**, *50*, 7238; c) S. Losse, J. G. Vos, S. Rau, *Coord. Chem. Rev.* **2010**, *254*, 2492.
[37] W. Zhang, J. Hong, J. Zheng, Z. Huang, J. Zhou, R. Xu, *J. Am. Chem. Soc.* **2011**, *133*, 20680.

